SINERGI Vol. 28, No. 2, June 2024: 327-336
http://publikasi.mercubuana.ac.id/index.php/sinergi
http://doi.org/10.22441/sinergi.2024.2.012

Effect of near-surface heterogeneities on the pore-water pressure distribution and slope stability

Nurly Gofar[1*], Ega Nanda Pangestika[1], Yudi Harianto[1,2], Herdian Gumay[3], Alfrendo Satyanaga[4]
[1]Department of Civil Engineering, Graduate Program, Universitas Bina Darma, Indonesia
[2]Geoteknik Pratama, Civi Engineering Laboratory, Indonesia
[3]Department of Civil Engineering, Faculty of Engineering, Universitas Hasanuddin, Indonesia
[4]Department of Civil and Environmental Engineering, Nazarbayev University, Kazakhstan

Abstract
Seepage and slope stability are important problems analyzed in geotechnical engineering. Conventionally, the analysis is performed in conditions where the soil is intact. However, near-surface soil is subjected to various conditions that lead to heterogeneity, for example, the presence of cracks in clay, relics in weathered rock, and plant roots. The presence of cracks and other forms of heterogeneity on the near-surface layer increases the rainfall infiltration into the slope and changes the pore water pressure distribution accordingly. Water infiltration increases the pore water pressure, raises groundwater level, and decreases the matrix suction of unsaturated soils - which is a critical factor for the stability of slopes. This study aims to evaluate the effect of varying permeability of near-surface soil on the rainwater infiltration to slope and, subsequently, the safety factor. In this case, the near-surface soil is modeled as a layer with higher permeability. Numerical analysis performed in this study using SEEP/W and SLOPE/W indicated that considering this condition results in a higher safety factor of the slope because the higher permeability resulting from heterogeneity helps dissipate pore water pressure, which is critical in maintaining the slope stability during heavy rainfall.

Keywords:
Heterogeneity;
Pore-water pressure;
Rainfall;
Slope stability;
Suction;

Article History:
Received: September 5, 2023
Revised: December 12, 2023
Accepted: January 3, 2024
Published: June 2, 2024

Corresponding Author:
Nurly Gofar
Civil Engineering Department,
Universitas Bina Darma,
Indonesia
Email:
nurly_gofar@binadarma.ac.id

INTRODUCTION

Rainfall-induced slope failure is a prevalent geohazard in tropical countries covered with residual soils and deep groundwater tables. The reduction in soil shear strength resulting from elevated pore water pressure and reduced matrix suction can result in slope failure. For example, rainfall-induced slope instability has been studied by [1, 2, 3, 4, 5]. The studies concluded that the stability of a slope is influenced mainly by the geometry of the slope, the soil characteristics, and the rainfall duration and intensity. The normal depth of the slip surface in rainfall-induced slope failures is between one and three meters, and it is aligned in a direction that is parallel to the slope surface. Thus, analytical analysis is usually carried out in the case of an infinite slope. Cracks at the crest or slope surface could initiate the slip surface. The presence and size of cracks are usually detected by visual observation or various methods outlined in [6].

Conventionally, slope stability analysis was performed for total and effective conditions whereby the soil is assumed to be in saturated condition. The application of the unsaturated soil mechanics concept was deemed to be difficult and time-consuming. However, the integration of computer programs enables the speedy execution of seepage and infiltration analysis in unsaturated soil, as well as the assessment of slope stability.

Rainfall-induced slope failures are primarily caused by complete or partial dissipation of matric suction within the unsaturated zone during rainfall infiltration,

which decreases the soil's shear strength [7]. The analysis of rainfall-induced slope instability is usually performed in conditions where the soil is intact and homogeneous.

In fact, the near-surface soil is subjected to various boundary conditions such as rainfall infiltration, evaporation, and transpiration. The effect of these boundary conditions was studied numerically by [8] and [9] and more extensively using field data by [10]. The studies concluded that both actual evaporation and rainfall significantly affect accurate factor of safety variations and pore-water pressure distribution within soil layers. The alternation of rainy and dry periods causes the development of desiccated cracks in clay [11][12] which lead to seepage concentration through the crack. Furthermore, the transient processes of pore water pressure distribution depend on the soil's hydraulic and mechanical properties and the geometry of the moving mass [13].

Besides the crack formation on the surface soil, the residual soil formation process in tropical regions introduces minor hydraulic heterogeneities on the soil surface, significantly influenced by preexisting discontinuities such as relic and core-stone [14][15]. Furthermore, the root of vegetation also introduces heterogeneity on the near-surface layer because roots uptake water from the soil, leading to variation in moisture around the root system with the distance between the trees and the soil [16]. Together, these three forms of heterogeneity had the potential to generate inconsistencies in the suction distributions, increase the rainfall infiltration into the slope, and subsequently decrease the suction. Figure 1 shows the slope surface, indicating some heterogeneities in the near-surface soil layer.
Considering the hydraulic heterogeneity of the near-surface soil is a complicated task. [17] showed that analyzing the effect the presence of a crack at the surface should not consider only the soil matrix part of the cracked soil, but also the crack network. The effects of relict discontinuities on the stability of residual soil slopes in tropical regions are also difficult due to the unpredictable hydrological influences and the intrinsic heterogeneity of the indigenous soils [18]. Based on their study, [16] concluded that trees contribute to slope stability both hydrologically as a result of the increase in matric suction of the soil resulting in an increase in the shear strength and mechanically due to root reinforcement.

Figure 1. Slope surface condition

To study the effect of relic-joint on soil permeability, [19] conducted a laboratory model test on intact soil and soil with different relic patterns. They found that the occurrence of relic and core stones in Grade V material causes the variability of saturated mass permeability of the residual soil range over one order of magnitude. Similarly, based on their research on the saturated coefficient of permeability of granitic residual soil in Bukit Timah, Singapore, [20] concluded that the saturated coefficient of permeability of the residual soil mantle varies within two orders of magnitude.

The impact of precipitation patterns on soils with varying permeability levels was investigated by [21] under conditions of delayed, regular, and advanced preceding rainfall patterns. The findings suggest that soil with low permeability is more susceptible to instability than soil with high permeability. Thus, modelling the heterogeneity in the near-surface soil as a soil layer with a higher coefficient of saturated permeability could lead to a more realistic evaluation of rainfall-induced instability.

This paper focuses on investigating the effect of near-surface soil heterogeneities on the transient pore water pressure induced by rainfall infiltration.

The heterogeneity is assumed to increase the permeability of the near-surface soil, thus; a higher permeability coefficient was used for the analysis while other properties were kept similar. Numerical analyses of soil slopes were performed under different rainfall scenarios i.e., high-intensity short-duration, low-intensity, long-duration, and a combination of antecedent and major rainfall. SEEP/W program was used to evaluate the transient pore-water pressure distribution in the soil during and after the rainfall scenarios. Furthermore, the slope stability analysis was carried out using the limit equilibrium method in SLOPE/W at any time by the limit equilibrium method to evaluate the change in the slope's safety factor during and after rainfall.

METHOD

The methodology adopted in this study is the numerical analysis of a slope found in the city of Pagar Alam, South Sumatra. Samples were collected to identify soil forming the slope. The geometry of the slope was estimated based on the field condition.

Study Location and Geometry of the Slope

Figure 2 shows the location of Pagar Alam city in South Sumatra Province. A slope in the South Sumatra National Road segment no 037, i.e. Simpang Air Dingin – Pagar Alam was selected for this study. The location coordinates are 4° 4'23.67" South Latitude and 103°19'26.47" East Longitude.

Figure 3 shows the geometry of the slope used in this study. The slope is inclined at 27° and has a height of 10 m. In this study, the near-surface soil is modeled as a 1-m thick layer with a coefficient of saturated permeability higher than the rest of the soil. In this article, the original soil is referred to as Soil 1 while the near-surface soil layer is called Soil 2a and Soil 2b.

Soil Properties

Disturbed samples were collected from a depth of 1 – 2 m. Disturbed samples were used to determine index properties and soil classification based on sieve analysis and Atterberg limits. Results of laboratory tests showed that according to ASTM D-2847, the soil forming the slope can be classified as clay with medium to high plasticity [22].

Deeper locations are required for undisturbed sampling in order to find an intact sample. The undisturbed samples were used to determine the saturated coefficient of permeability and the effective shear strength of the soil.

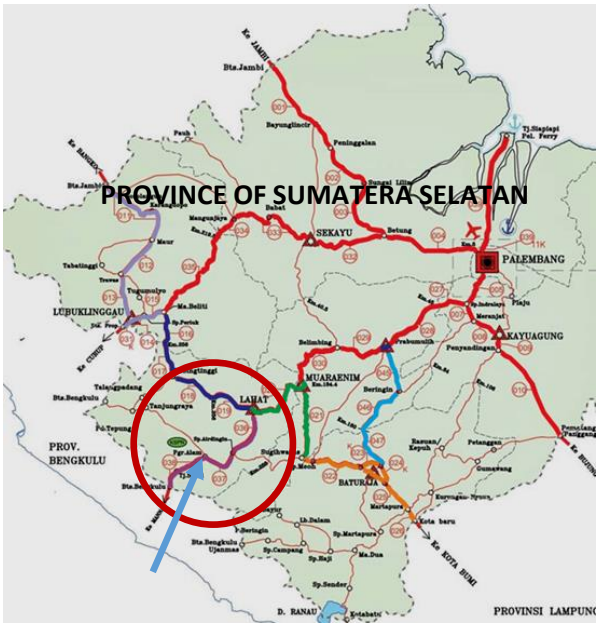

Figure 2. Study Location

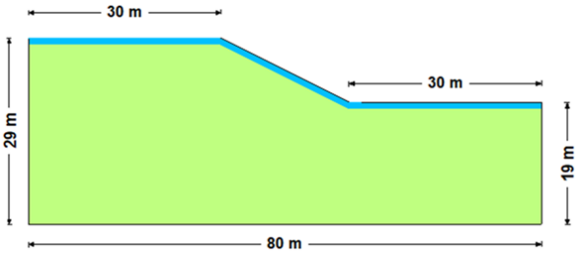

Figure 3. Geometry of the slope

The coefficient of saturated permeability of the soil is 4.5×10^{-6} (m/s). The properties of the soil selected for this study are summarized in Table 1.

Table 1. Soil Properties

Properties	Unit	Soil 1	SNI
Specific gravity (*Gs*)		2.62	SNI 1964-2008
Porosity (*h*)		0.62	calculation
Saturated coef. of permeability (k_{sat})	m/s	4.5×10^{-6}	SNI 03-6870:2002
Passing No 200 sieve (*w*)	%	56.39	SNI-ASTM C117-2012
Liquid Limit (*LL*)	%	52.3	SNI 1967-2008
Plasticity Index (*PI*)	%	27.13	SNI 1966-2008
Soil Classification		CH	SNI 6371-2015
Cohesion *c'*	kPa	5	SNI 2813-2008
Internal friction angle ϕ'	o	21	
Rate of increase in internal friction angle due to suction ϕ^b	o	14	Correlation $\phi^b = 2/3\phi'$

Soil Water Characteristic Curve (SWCC) and permeability function are two primary soil properties used in the analysis of pore water pressure variation in soil. A straightforward estimation of SWCC for plastic soil based on the grain-size distribution and the plasticity index (PI) [23] was adopted in this study. This method is used to calculate parameters a, n, m in the Fredlund and Xing fitting equation of SWCC [24].

$$\theta(\psi,a,n,m) = C(\psi) * \frac{\theta_s}{\left\{ln\left[e+\left(\frac{\psi}{a}\right)^n\right]\right\}^m} \quad (1)$$

whereas a, n, m are unknown fitting parameters, ψ is the matric suction = (u_a-u_w), θ_s is the saturated water content, e is the natural number (≈2.72) and $C(\psi)$ is a correction factor defined as follows:

$$C(\psi) = \frac{ln\left(1+\frac{\psi}{\psi_r}\right)}{ln\left[1+\left(\frac{1'\ 000'\ 000}{\psi_r}\right)\right]} + 1 \quad (2)$$

The parameter ψ_r is a fitting parameter related to the residual suction. In this case ψ_r =500 should give a good prediction of SWCC [25]. Zapata method predicts the shape of SWCC based on a weighed Plasticity index, *wPI* for non-plastic soils, whereby w and *PI* is the percentage of particle passing No 200-sieve expressed in decimal and the plasticity index expressed as percentage respectively. Parameters a, n, and m are calculated using (3), (4) and (5).

$$a = 32.835\ \{ln(wPI)\} + 32.438 \quad (3)$$

$$n = 1{,}421\ (wPI)\text{-}0.3185 \quad (4)$$

$$m = -0.2154\{ln(wPI)\} + 0.7145 \quad (5)$$

The SWCC used in this study is presented in Figure 4. The permeability function calculated using Fredlund et al. [26] fitting equation integrated in SEEP/W based on the coefficient of saturated permeability and SWCC is shown in Figure 5. The coefficient of saturated permeability was obtained using a falling head test following SNI 03-6870:2002.

In this study, Soil 2 was assumed to have the same properties as Soil 1. Only the coefficient of saturated permeability of the near surface layer was increased by one order of magnitude (Soil 2a) and two orders of magnitude (Soil 2b) to account for the heterogeneity of the near-surface soil.

The extended Mohr-Coulomb shear strength envelope for unsaturated soils requires that three shear strength parameters be defined namely, c', ϕ' and ϕ^b. The c' and ϕ' parameters can be measured using standard laboratory equipment on saturated soil specimens.

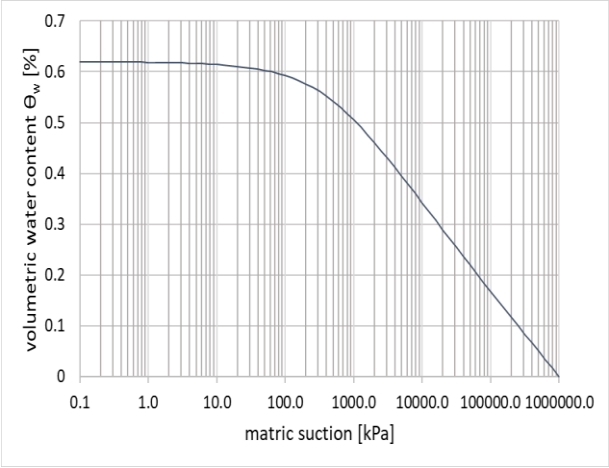

Figure 4. SWCC of soil forming the slope (soil 1)

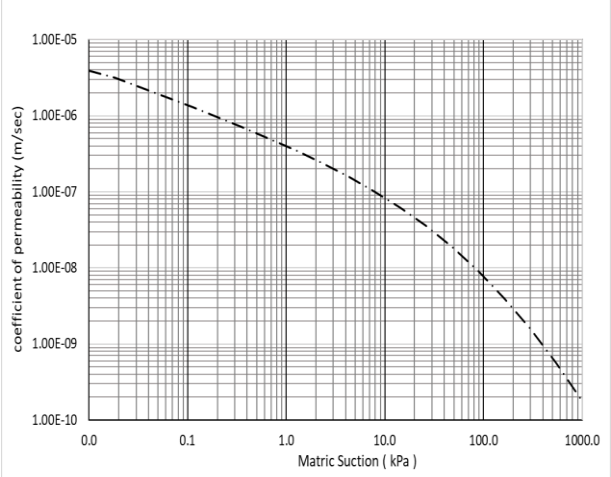

Figure 5. Permeability curve of the soil 1

However, conventional triaxial and direct shear equipment require modifications before testing unsaturated soils, i.e., measuring the ϕ^b. In this study, the shear strength of the unsaturated soil was estimated based on a direct shear test (SNI 2813-2008) on undisturbed samples collected on the site from a depth of 2 m. The direct shear test resulted in the effective cohesion (c') of 5 (kPa), effective internal friction angle (ϕ') of 21^{o,} and rate of increase in internal friction angle with suction or ϕ^b = 2/3 ϕ' = 14^o [27].

Rainfall Record

The daily rainfall data was collected from Pagar Alam PTPN VII Rainfall Station. Figure 6 presents the annual rainfall data in this area from 1985 to 2021. The average annual rainfall recorded was 2767 (mm) with a standard deviation of 796 mm. The annual rainfall of more than 2000 (mm) is considered very high even in the tropical rainforest, thus rainfall-induced slope failures and flash floods are normal occurrences in this area. Observation of the daily rainfall data

from 1985 to 2021 yields the maximum daily rainfall was 219 (mm) in 2001, and the maximum 5-day rainfall was 362 (mm), also in 2001, while the maximum monthly rainfall was 861 (mm) in 2009.

Based on this data, three rainfall scenarios were designed. The first scenario was the high-intensity short-duration rainfall of 220 (mm/day) which lasted for 10 hours resulting in 22 (mm/hr) for 10 hours. The second scenario was 861 (mm) of rain for 30 days resulting in a low-intensity long-duration rainfall of 1.17 (mm/hr) for 30 days. The third scenario was the combination of antecedent rainfall and major rainfall which was selected based on the results of scenario 2.

The analysis was carried out for 27º slope angle in three conditions. The first case assumes a homogeneous soil forming the slope while the second and the third cases consider the homogeneity in the near-surface soil by varying the coefficient of saturated permeability of the soil near the ground surface. The near-surface soil (soil 2) is 1-m thick with the same soil properties as Soil 1 but a higher coefficient of permeability. The saturated permeability was set as one order of magnitude (Soil 2a) and two orders of magnitude (Soil 2b) higher than the rest of the soil. The matrix of analyses is displayed in Table 2.

In the first analysis (A), rainfall with an intensity of 22 (mm/hr) or 6.1×10^{-6} (m/s) applied for 10 hours was used for the seepage analysis, while slope stability analysis was carried out at the interval of 1 hour from the start of rainfall application up to 1 day (24 hours). The second analysis (B) is by applying rainfall of 1.17 (mm/hr) or 3.24×10^{-7} (m/s) for 30 days, while slope stability analysis was carried out at the interval of 1 day from the start of rainfall application up to 1 month (30 days). The third analysis (C) was aimed at evaluating the effect of antecedent rainfall. In this case, initial suction is created by applying rainfall of 1.17 (mm/hr) or 3.24×10^{-7} (m/s) for a number of days (based on the analysis in Scenario 2 and the criteria for slope stability given in SNI 8460-2017 [22] i.e., Factor of Safety ≥ 1.5.) before applying heavy rainfall with the intensity of 22 (mm/hr) or 6.1×10^{-6} (m/s) for 10 hr.

Numerical Analysis

Numerical modeling was carried out to investigate the factor of safety of the selected slope in Pagar Alam. The finite element analysis was conducted for transient seepage analysis using SEEP/W, followed by slope stability analysis using SLOPE/W at some designated times [28]. The present analytical approach assesses the effect of heterogeneity in the near-surface soil by adopting a soil layer with higher permeability.

Figure 7 shows the simplified model of the slope inclined at an angle of 27° and height of 10 (m). Left and right boundary conditions were placed at three times the height of the slope. A hydrostatic initial condition was set based on the position of the groundwater table as shown in the figure. The left and right edges above the water table were specified as no-flow boundaries (Q=0), while the edges below the water table were assigned as head boundaries with pressure heads equal to the vertical distance from the water table. These boundary conditions were necessary for enabling lateral flow to take place within the saturated zone. The bottom boundary was located 19 m from the ground surface at the toe and was assumed as an impermeable layer (no flow). The initial suction was set based on the position of the groundwater table.

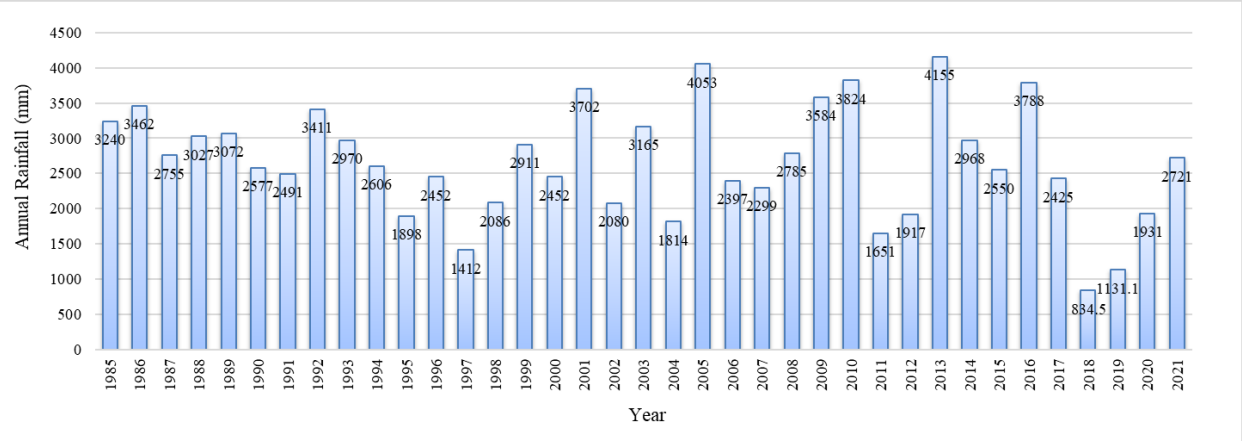

Figure 6. Annual rainfall in Pagar Alam

Table 2 Matrix of analysis

Case	Slope angle	Soil	Rainfall scenario	Antecedent rainfall	Major Rainfall
1	27°	1 soil layer	A	No	22mm/hr. applied for 10 hr.
			B	1.17 mm/hr. for 30 days	No
			C	1.17 mm/hr. for *)	22mm/hr. applied for 10 hr.
2	27°	2 soil layers	A	No	22mm/hr. applied for 10 hr.
		Soil 2 with	B	1.17 mm/hr. for 30 days	No
		k_{sat} = 4.5 × 10^{-5} m/s	C	1.17 mm/hr. for *)	22mm/hr. applied for 10 hr.
3	27°	2 soil layers	A	No	22mm/hr. applied for 10 hr.
		Soil 2 with	B	1.17 mm/hr. for 30 days	No
		k_{sat} = 4.5 × 10^{-4} m/s	C	1.17 mm/hr. for *)	22mm/hr. applied for 10 hr.

*) The duration of 1.17mm/hr rainfall for rainfall scenario 3 was based on the results of analysis for Case 2

RESULTS AND DISCUSSION

Transient Pore-water Pressure Distribution

The pore water pressure distribution is presented as a function of depth for cross-section A-A (Figure 7). Before rainfall (t = 0) the distribution of pore-water pressure is hydrostatic i.e., zero at the groundwater level. For this cross-section, the elevation of the groundwater level is 16m from the datum. Before rainfall, the suction at the surface is set at -100 kPa.

The pore water pressure distribution during major rainfall application in Scenario A is shown in Figure 8. It can be seen from Figure 8a that for Case 1, rainfall of 22 (mm/hr) for 10 hours only wets the soil surface until it is saturated at 10 hours but water did not infiltrate into the soil. Thus, for scenario A, rainfall did not cause slope failure as the initial suction was very high. The presence of a near-surface layer with higher permeability (Case 2, Soil 2a) caused the water to infiltrate into soil 2 and was retained in this layer (Figure 8b).

Variation in Factor of Safety

The change in the factor of safety (FOS) for rainfall scenario A is shown in Figure 10. It can be seen from the figure that the FOS decreases with the application of rainfall from 2.388 to 2.333. The FOS continued to decrease even after the rainfall stopped. Thus, high intensity and short-duration rain does not cause slope failure in this area where the soil forming the slope is CH.

The presence of heterogeneity in the near-surface soil modeled by increasing the saturated permeability by one order of magnitude (Soil 2a), increases the initial FOS. The FOS decreased from 2.408 to 2.344 during the 10-hour rainfall. However, when the saturated permeability was increased by two orders of magnitude (Soil 2b) the FOS decreased significantly from 2.408 to 2.239. The most significant reduction of FOS was from 9 to 10 hours because at this point infiltration has reached the groundwater table.

SNI 8460-2017 suggested that for slope when results of soil investigation are unreliable, the factor of safety (FOS) of 1.5 should be used. as design value. In this case, the major rainfall (Scenario 1) cannot lead to slope failure both in Case 1 and Case 2. The lowest FOS (2.239) was obtained for Case 3, where the near-surface soil was modeled as a 1-m thick layer with a coefficient of saturated permeability two orders of magnitude higher than the original soil (Soil 2b).

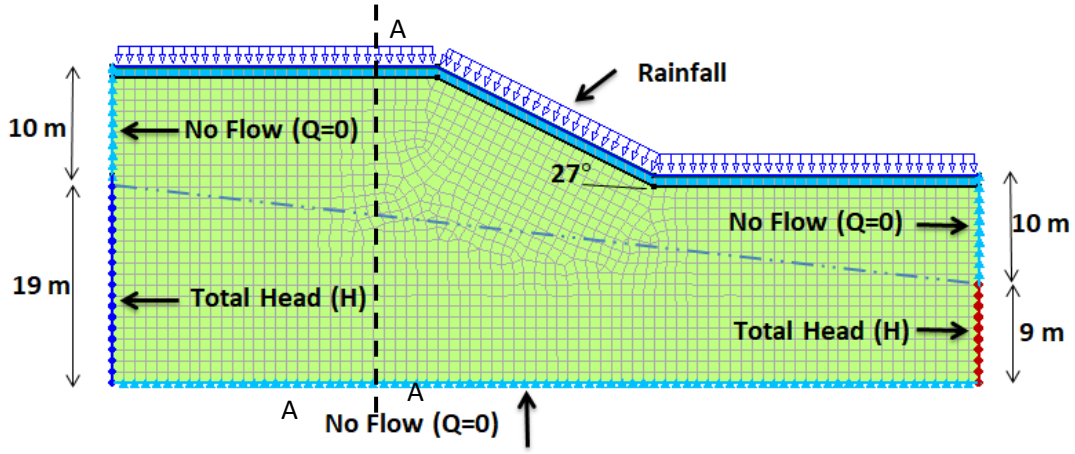

Figure 7. Slope model and boundary conditions for seepage analysis

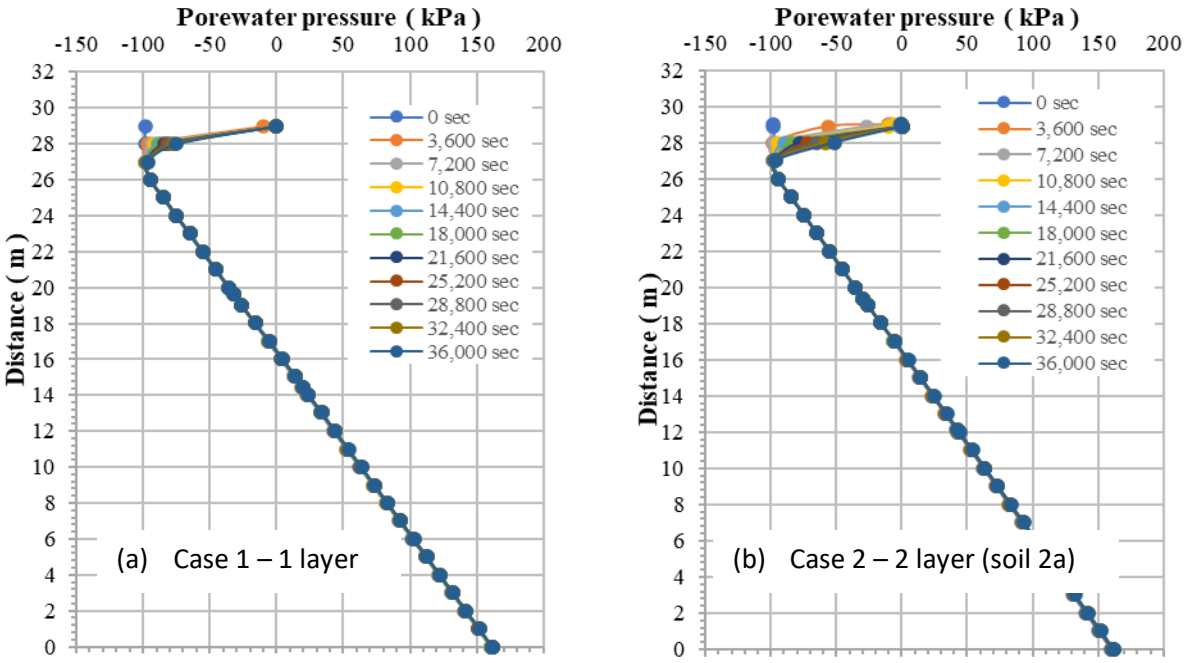

Figure 8. Porewater pressure distribution due to rainfall scenario A

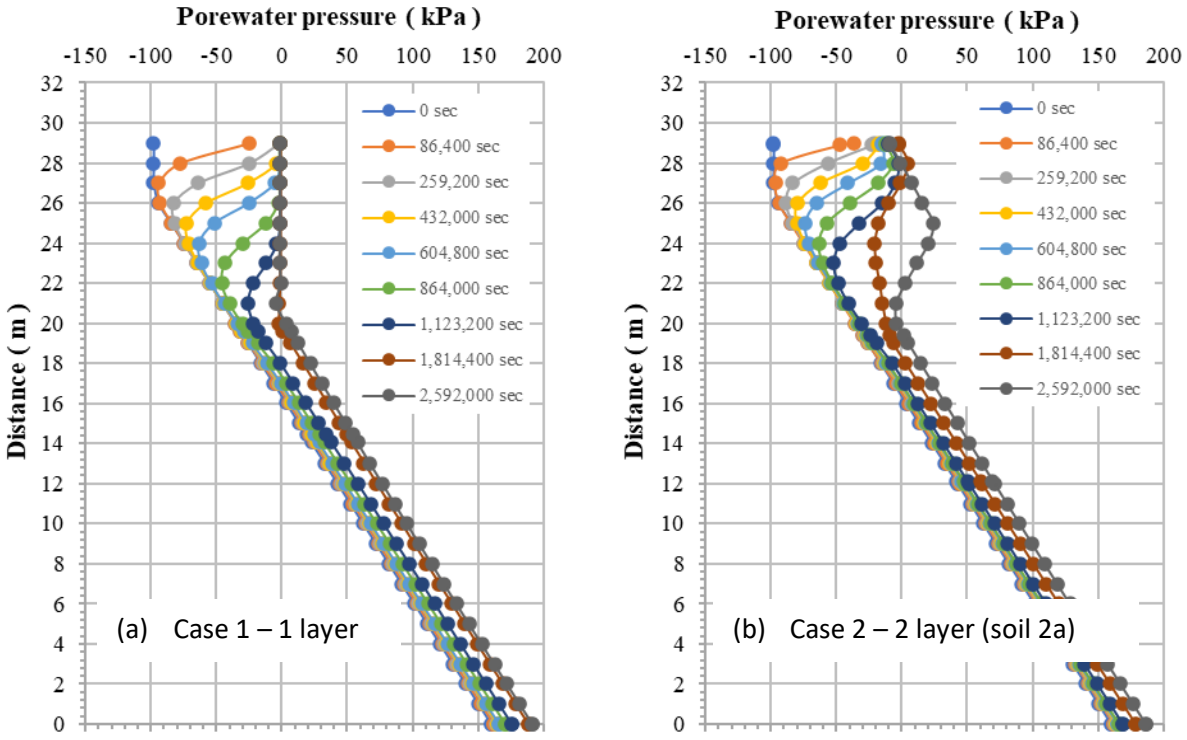

Figure 9. Porewater pressure distribution due to rainfall scenario B

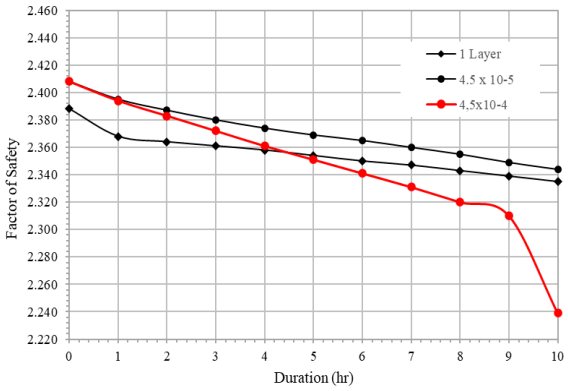

Figure 10. Change in safety factors of slope subjected to high-intensity short-duration rainfall.

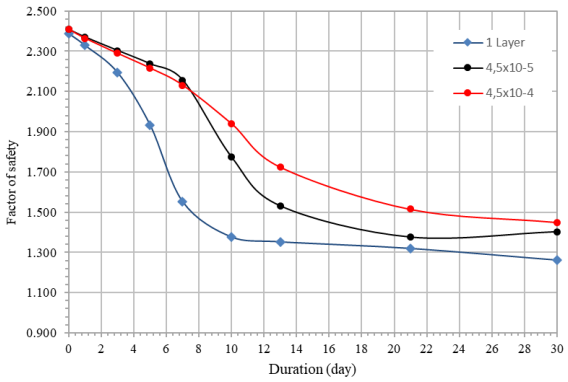

Figure 11. Change in safety factors of slope subjected to low-intensity long-duration rainfall

The change in the FOS for rainfall scenario B is shown in Figure 11. It can be seen from the figure that the Factor of safety (FOS) decreases with the application of rainfall from 2.388 to 1.261 due to the low-intensity long-duration rainfall for 30 days. The FOS continued to decrease even after the rainfall stopped. If the heterogeneity in the near-surface soil is modeled by the coefficient of saturated permeability one order of magnitude higher (Soil 2a), the safety factor decreased from 2.408 to 1.402, which is slightly higher than the safety factor for one layer. Further increase in the coefficient of saturated permeability (Soil 2b) caused a further increase in FOS. Thus, rain with low-intensity and long-duration can cause the failure of the slope where the soil forming the slope is CH but the presence of heterogeneity in the near-ground surface increases the FOS thus delaying the failure.

The long-duration rainfall creates enough moisture to reduce the soil's shear strength and lead to slope failure. From Figure 10, we can see that for 1-layer soil, the FOS = 1.5 was reached after about 7 days of rainfall.

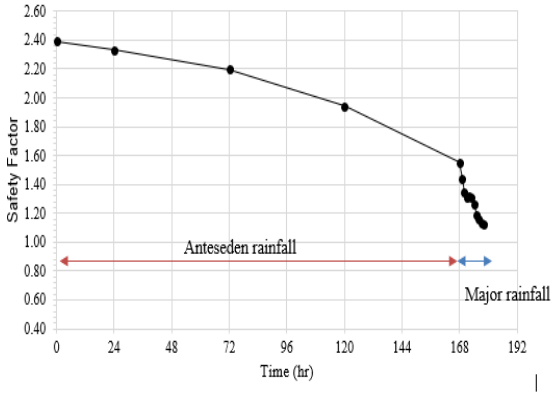

Figure 12. Change in safety factors for Case 1 slope subjected to rainfall scenario C

The higher coefficient of saturated permeability in the near-surface layer by one order of magnitude increased the duration needed to reach FOS = 1.5 in 13 days while increasing the coefficient of saturated permeability by 2 orders of magnitude increased the FOS, thus FOS = 1.5 was reached only after 22 days of rainfall.

Figure 12 shows the effect of the combination of antecedent rainfall for 7 days and major rainfall for 10 hours on a slope modeled as 1 soil layer (rainfall scenario C on Case 1). The FOS decreased from 2.408 to 1.551 due to antecedent rainfall; then, decreased further to 1.122 due to 10 hours of heavy rainfall. At this point, the slope is considered to have failed. Longer durations of antecedent rainfall i.e. 14 days and 21 days were required for cases 2 and 3 respectively.

Discussion

The results obtained in this study are comparable with the previous study [4] that for slopes made of high-plasticity soil, the slope failure is initiated by long-duration rainfall. The subsequent heavy rainfall triggers the failure because the porosity of the soil has been filled with water from the preceding rainfall. The higher the permeability of surface soil, the faster the water infiltration and the lower the factor of safety. The results agree with the study by [3] that antecedent rainfall plays an important role in initiating rainfall-induced slope failure. However, the duration of antecedent rainfall is affected by the slope surface condition.

CONCLUSION

Based on the results obtained from the finite element analysis of transient water flow and slope stability, the following conclusions were drawn:

1. Heavy rain lasting for 10 hours does not cause slope failures because the soil is initially still dry. The rainfall only wets the surface of the soil without seeping in. The lowest FOS (2.239) was obtained when the near-surface layer was modeled as a material with a coefficient of saturated permeability 4.5 x 10^{-4} m/s (two orders of magnitude higher than the original soil)
2. Prolonged events with less intense rainfall critically reduce the stability of the slope. The FOS decreased from 2.408 to less than 1.5 for all cases. This reduction in the FOS is due to the increase in pore water pressure and the reduction in matric suction, which contributes to the reduction in soil strength. The lowest FOS (1.261) was obtained for the case 1.
3. Non-uniformity of the surface soil has an effect on changes in the transient pore water pressure. Modeling of heterogeneities of near-surface soil by assuming a soil layer with higher permeability can effectively predict pore water pressure distribution in the soil. However, the effect on the FOS is not conclusive, especially when a higher coefficient of saturated permeability is used.
4. For slopes formed by clay with high plasticity, the rainfall pattern with antecedents provides critical conditions because the antecedent rain causes the soil to become moist and the water absorption capacity becomes smaller, thus high-intensity rain that follows the antecedent rainfall can cause slope failures.

ACKNOWLEDGMENT

This research was partially supported by Universitas Bina Darma Internal Funding 2022.

REFERENCES

[1] L. L. Zhang, J. Zhang, L. M. Zhang, and W. H. Tang," Stability analysis of rainfall-induced slope failure: a review," *Proceedings of the ICE - Geotechnical Engineering 2011*, 2011, vol. 164, no. 5. pp. 299-316, doi: 10.1680/geng.2011.164.5.

[2] T. Yoshikawa, and T. Noda, "Numerical analysis on failure mechanism of unsaturated slope due to rain," in *Smart Geotechnics for Smart Societies,* Zhussupbekov, Sarsembayeva & Kaliakin (Eds) ISBN 978-1-003-29912-7 Open Access: www.taylorfrancis.com, 2023.

[3] H. Rahardjo, MM. Nistor, N. Gofar, A. Satyanaga, X. Qin, S.I.C. Yee, "Spatial distribution, variation and trend of five-day antecedent rainfall in Singapore," *Georisk: Assessment and Management of Risk for Engineered Systems and Geohazards,* vol. 14, no. 3, pp. 177-191, 2020, doi: 10.1080/17499518.2019.1639196

[4] N. Gofar, and M. L. Lee, "Extreme Rainfall Characteristics for Surface Slope Stability in the Malaysian Peninsular," *Georisk: Assessment & Management Risk for Engineering Systems & Geohazards,* vol. 2, no. 2, pp. 65-78, 2009, doi: 10.1080/17499510802072991

[5] Y. Yuliastuti et al., "The assessment of drainage performance in the residential area using SWMM," *SINERGI*, vol. 27, no. 2, pp. 281-288, 2023, doi: 10.22441/sinergi.2023.2.016

[6] R. Lionnie, R.C. Ramadhan, A.S. Rosyadi, M. Jusoh. M. Alaydrus," Performance analysis of various types of surface crack detection based on image processing," *SINERGI,* vol. 26, no. 1, pp. 1-6, 2022, doi: 10.22441/sinergi.2022.1.001

[7] D. G. Fredlund, H. Rahardjo, and M. D. Fredlund, *Unsaturated Soil Mechanics in Engineering Practice,* John Wiley & Sons, Inc. 2012.

[8] F.O. Augusto, M.A. Fernandes, "Landslide analysis of unsaturated soil slopes based on rainfall and matric suction data," *Bulletin of Engineering Geology and Environment, vol.* 78, pp. 4167–4185, 2019, doi: 10.1007/s10064-018-1392-5.

[9] G. H. Yunusa, A. Kassim, and N. Gofar. "Effect of surface flux boundary conditions on transient suction distribution in homogeneous slope," *Indian Journal of Science and Technology,* vol. 7, no. 12, pp. 2064, 2014, doi: 10.17485/ijst/2014/v7i12.23

[10] N. Gofar, A. Satyanaga, R. Y. Tallar, and H. Rahardjo, "Role of actual evaporation on the stability of residual soil slope," *Geotechnical and Geological Engineering,* vol. 40, no. 9 pp. 4585-4594. 2022, doi: 10.1007/s10706-022-02172-z

[11] S. Krisnanto, H. Rahardjo, R.D. Kartiko, A. Satyanaga, J. Nugroho, N. Mulyanto, P., Santoso, A. Hendiarto, D. B. Pamuji, S. N. Rachma, "Characteristics of Rainfall-Induced Slope Instability at Cisokan Region", *Indonesia. Journal of Engineering and Technological Sciences* (JETS), vol. 53, no. 5, pp. 210504, 2021, doi: 10.5614/j.eng.technol.sci.2021.53.5.4

[12] M. Mukhlisin, K.N. Khiyon, "The Effects of Cracking on Slope Stability," *Journal of Geological Society of India*, vol. 91, pp. 704–710, 2018, doi: 10.1007/s12594-018-0927-5

[13] Di Maio, J. De Rosa, R. Vassallo, "Pore water pressures and hydraulic conductivity in the slip zone of a clayey earthflow:

Experimentation and modeling," *Engineering Geology,* vol. 292, ID: 106263, 2021, doi: 10.1016/j.enggeo.2021.106263

[14] R. Ullah, R.A. Abdullah, A. Kassim, N.Z.M. Yunus, H. Sendo," Assessment of Residual Soil Properties for Slope Stability Analysis," *International Journal of GEOMATE,* vol. 21, no. 86, pp. 72-80, 2021, doi: 10.21660/2021.86.j2282

[15] A. Kassim, N. Gofar, M. L. Lee and H. Rahardjo "Modeling of Suction Distribution in an Unsaturated Heterogeneous Residual Soil Slope" *Engineering Geology,* vol. 1310132, pp. 70-82, 2012, doi: 10.1016/j.enggeo. 2012.02.005.

[16] N. Ali, I. Farshchi, M. A. Mu'azu, and S. W. Rees "Soil-root interaction and effects on slope stability analysis," *Electronic Journal of Geotechnical Engineering,* vol. 17, pp. 3019-328, 2012.

[17] S. Krisnanto, & H. Rahardjo," Advancement in the Analysis of Seepage through Cracked Soils," *Journal of Engineering and Technological Sciences,* vol. 50, no. 4, pp. 566-577, 2018, doi: 10.5614/j.eng.technol. sci.2018.50.4.8

[18] S. Hencher, A. Malone, "Hong Kong landslides," In book: *Landslides: Types, Mechanisms, and Modeling,* Chapter 30, pp. 373-382, Clague & Stea (Eds), 2012, Cambridge University Press, doi: 10.1017/CBO9780511740367.031.

[19] N. Gofar, A. Kassim, and M. L. Lee. "Effect of Relict Joint on The Mass Permeability of Residual Soil," *Proceedings of Geotechnical Engineering for Disaster Mitigation and Rehabilitation and Highway Engineering,* 2011*,* pp. 374-379.

[20] T.V. Bharat and J. Sharma, "Validity limits of Fredlund–Xing–Kunze model for the estimation of hydraulic properties of unsaturated soils," In *Proceedings of the Canadian Geotechnical Conference*, Winnipeg, 2012, Paper No. 263, doi: 10.1016/j.enggeo.2004.12.001

[21] A. Rahimi, H. Rahardjo, and E. C. Leong, "Effect of hydraulic properties of soil on rainfall-induced slope failure," *Engineering Geology,* vol. 114, no. 3-4, pp. 135–143, 2010, doi: 10.1016/j.enggeo.2010. 04.010.

[22] ASTM Standard D 2487- 2017 *Standard Practice for Classification of Soils for Engineering Purposes (Unified Soil Classification System)* ASTM International, West Conshohocken, PA, 2003. www.astm.org.

[23] A. Satyanaga, A.S., Mohammad, A.B., Ibrahimi, M., Wijaya, S.W. Moon, J. Kim, "Direct and indirect methods in determination of water retention curve of residual soils," in *Smart Geotechnics for Smart Societies,* Zhussupbekov, Sarsembayeva & Kaliakin (Eds) ISBN 978-1-003-29912-7 Open Access: www.taylorfrancis.com.

[24] N. Gofar, and H. Rahardjo, "Saturated and Unsaturated Stability Analysis of Slope Subjected to Rainfall Infiltration," *MATEC Web of Conferences 101, 05004-Sriwijaya International Conference on Engineering, Science and Technology (SICEST2016).* 2017*,* doi: 10.1051/matecconf/ 201710105004

[25] F, Zhang and D.G. Fredlund, "Examination of the estimation of relative permeability for unsaturated soils," *Canadian Geotechnical Journal*, vol. 52, no. 12, pp. 2077-2087, 2015, doi: 10.1139/cgj-2015-0043

[26] N. Gofar, and H. Rahardjo, "Saturated and Unsaturated Stability Analysis of Slope Subjected to Rainfall Infiltration," *MATEC Web of Conferences SICEST 2016,* Bangka Island, Indonesia, 2016, vol. 101, no. 11, pp. 05004, doi: 10.1051/matecconf/ 201710105004

[27] Indonesia National Standardization Agency, Geotechnical *Design Requirements*, SNI 8460: 2017.

[28] *GEOSTUDIO User's Manual*, 2018, Geo-Slope International Ltd, Calgary, Alberta, Canada.